Virchows Arch (1997) 431:53–61

ORIGINAL ARTICLE

Yoshihide Fujigaki · Mitsumasa Nagase
Kenichiro Kojima · Tatsuo Yamamoto · Akira Hishida

Glomerular handling of immune complex in the acute phase of active in situ immune complex glomerulonephritis employing cationized ferritin in rats

Ultrastructural localization of immune complex, complements and inflammatory cells

Received: 26 November 1996 / Accepted: 10 February 1997

Abstract The ultrastructural localization of immune complex (IC) and inflammatory mediator systems in the glomerulus was investigated in active in situ IC glomerulonephritis employing cationized ferritin in rats. Glomerulonephritis was induced by unilateral renal perfusion of cationized ferritin as antigen (Ag) in preimmunized rats, and anti-ferritin antibody (Ab), C3 and the rat C5b–9 complex were localized by means of immunogold electron microscopy. Ag–Ab complexes were initially formed subendothelially, associated with C3, and attracted platelets, polymorphonuclear leucocytes (PMN) and monocytes. Then Ag–Ab complexes, without C3, passed across the glomerular basement membrane to re-aggregate subepithelially accompanied by C3 deposition after 1 day. Ag–Ab complexes without C3 accumulated in the inter-podocyte space within 1 day and were seen in the epithelial cells at 6 h. C5b–9 complexes were found in subepithelial immune deposits and in membrane vesicles of the epithelial cells, but only in very small amounts in subendothelial immune deposits. Accumulated platelets, PMN, and monocyte were in direct contact with endothelial cells or subendothelial IC. PMN and monocytes contained Ag, Ab and C3 in intracytoplasmic vacuoles. Ag–Ab complexes were also found in the mesangial matrix adjacent to the subendothelial region after 2 h and increased slightly in number, with expansion of the mesangial area thereafter. Most ICs formed in the subendothelial space rapidly formed lattices of a size that activated C3 and were then translocated to the subepithelial space. The potential ability of C3 to solubilize ICs in the subendothelial region may be important in this process. Endocytosis of subendothelial ICs by PMN and/or monocytes and the movement of ICs to the mesangial matrix may also contribute to the removal of IC from the subendothelial space.

Key words In situ immune complex formation · Glomerulonephritis · Complement · Membrane attack complex · Inflammatory cell

Y. Fujigaki (✉) · A. Hishida
First Department of Medicine,
Hamamatsu University School of Medicine, Handa-cho 3600,
431-31 Hamamatsu, Japan
Tel.: (81) 53-435-2261, Fax: (81) 53-434-9447

M. Nagase · K. Kojima
First Department of Medicine,
Teikyo University School of Medicine, Tokyo, Japan

T. Yamamoto
Division of Internal Medicine,
Seirei Hamamatsu General Hospital, Hamamatsu, Japan

Introduction

Subepithelial immune deposits in in situ immune complex (IC) nephritis induced by means of a cationic antigen are initially formed in the subendothelial region [10, 30]. The mechanisms for the translocation of subendothelial deposits to the subepithelial space and the mediators that contribute to this translocation are not well defined. The fate of those deposits that are not translocated to the subepithelial space is not well documented.

In IC-mediated glomerulonephritis, various mediator systems are involved in the induction of immunological glomerular damage. The activation of mediators occurs mainly when IC is located on the subendothelial side of the glomerular basement membrane (GBM), where cellular and humoral mediators can easily gain access to IC [9, 24]. Secondary mediators of inflammation might initiate and/or potentiate IC deposition in the GBM by enhancing glomerular permeability [1, 2]. Mononuclear and polymorphonuclear leucocytes (PMN) can function as phagocytic scavengers to eliminate immune reactants [5, 26, 28].

In passive in situ IC nephritis with cationized ferritin (CF) used as antigen (Ag), we have shown that IC is initially formed in the subendothelial region, activates C3, traverses the GBM as small IC units, then re-aggregates in the subepithelial space accompanied by C3 deposition [10]. The depletion of complement decreases the translo-

cation of ICs in passive in situ IC nephritis [11], suggesting that the complement system promotes an effective transfer of IC across the GBM, probably due to the solubilizing effect of complement on IC lattices [8, 20].

The C5b–9 membrane attack complex of complement has been recognized as a major mediator of IC-mediated glomerular injury through glomerular epithelial cell damage [6, 7, 15]. However, the formation and the role of C5b–9 complex in the subendothelial region of the GBM is poorly understood. Because C3 is activated in the subendothelial region, we have examined whether the membrane attack complex is also formed in the subendothelial region.

The mechanisms for the translocation of ICs and the contribution of complement to this translocation have not been studied in other models of IC-mediated glomerulonephritis. We examined how subendothelial deposits translocated to the subepithelial space in active in situ IC nephritis induced with CF and the contribution of C3 and the C5b–9 complex to this translocation. In addition we explored the role of infiltrating cells in the clearance of subendothelial deposits that were not translocated.

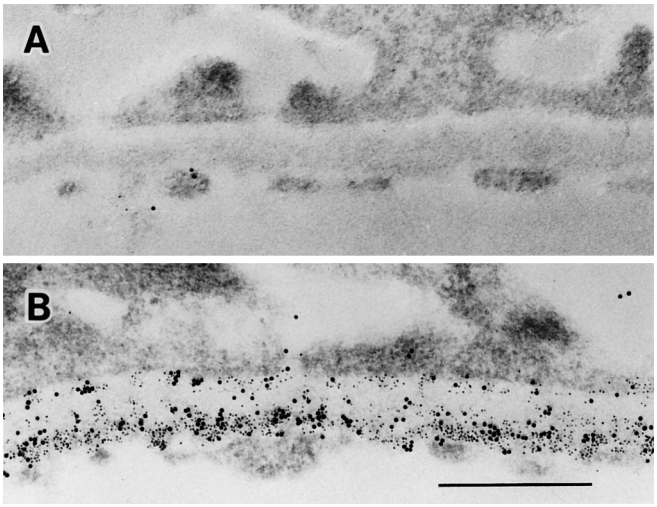

Fig. 1A, B Localization of rat IgG. ×40,000, *bars* 0,5 μm. **A** No rat IgG is labelled in the GBM of negative control rats in which PBS alone was perfused, without cationized ferritin injection. **B** Note distribution of rat anti-ferritin Ab (large particles) and ferritin (small particles) in the GBM is essentially similar in nephritic rats at 2 h, regardless of perfusion with PBS (cf. Fig. 2B)

Materials and methods

Active in situ IC glomerulonephritis was induced in 30 male Wistar rats of 100–120 g body weight (Japan SLC, Shizuoka, Japan), which were preimmunized with s.c. injections of 500 μg native ferritin (Sigma Chemical, St. Louis, Mo.) in Freund's complete adjuvant. Twenty-one days later, 25 rats were each anaesthetized with an i.p. injection of sodium pentobarbital (Nembutal, 50 mg/kg), and the abdominal cavity was opened by a midline incision. Microvascular clamps were placed on an aorta above and below the left renal artery. The left kidney was perfused with 0.5 ml of warm (37°C) phosphate-buffered saline (PBS), pH 7.4, through a needle placed in the aorta below the left renal artery, followed by 0.5 ml of PBS containing 500 μg CF (Sigma), and finally 0.5 ml of PBS at a constant rate of 0.5 ml/min. The whole procedure was carried out in less than 6 min. Blood flow was then restored to the left kidney. The times cited below are reckoned from the restoration of left renal arterial blood flow after the perfusion in nephritic rats.

Urine was collected in metabolic cages, and 24-h urinary protein excretion was estimated using Coomassie Brilliant Blue G-250 (Wako Pure Chemical Industries, Osaka, Japan) [3].

It is possible that the localization of soluble endogenous IgG or infiltrating cells might be affected by fixation procedures. To compare the influence of the fixation procedures on the distribution of endogenous IgG (both immune and non-immune IgG) in glomeruli, both immersion and perfusion fixations were performed in three preimmunized, non-Ag-perfused rats and two nephritic rats at each time point. For immersion fixation, the left kidney was trimmed and cut into small pieces and then immersed in 4% paraformaldehyde in 0.1 M phosphate buffer (pH 7.4) for 4 h at 4°C. For perfusion fixation, a catheter was inserted into the distal abdominal aorta and the aorta was clamped above the left renal artery. Shortly after perfusion was started, the aorta was clamped below the renal arteries and the inferior vena cava was cut. PBS was first perfused retrogradely for 2 min, and then 4% paraformaldehyde was perfused at 120 mmHg for 10 min, for immunoelectron microscopy (to detect rat IgG). Tissue was immersed in the same fixative for 4 h at 4°C.

In glomeruli fixed by perfusion in preimmunized, non-CF-perfused rats, the GBM was not labelled for rat IgG (Fig. 1A), suggesting that neither non-immune nor immune IgG has any affinity for the GBM. Qualitatively, the labelling pattern for rat IgG in the GBM and in the mesangium was essentially the same in nephritic rats fixed by perfusion as in rats fixed by immersion (Fig. 1B). This suggests that labelled rat IgG in the GBM or in the mesangium can be considered to be a constituent of IC interacting with the GBM or the mesangial matrix, and that the fixation procedure does not seriously affect the localization of IgG in the GBM or in the mesangium. Since glomerular infiltrating cells not directly adherent to the glomeruli may be removed by perfusion fixation, the immersion fixation method was adopted in this study.

In nephritic rats, following immersion fixation the distribution of labelled IgG varied among the capillary loops of the glomerulus, possibly because of leakage of plasma proteins from the capillary lumen during the fixation procedure. The labelling of IgG on the inner side of the GBM was somewhat dependent on the amount of plasma protein in the corresponding capillary lumina. Since pronounced leakage of plasma protein affects the distribution of IC and cellular blood components in glomeruli, only glomerular tufts revealing labelled IgG in the capillary lumen were chosen for investigation.

After the induction of nephritis, 2 or 3 rats were sacrificed at 15 min, 2 h, 6 h, and 1, 2, and 7 days. Two rats not given CF were used as controls 21 days after preimmunization. Left renal cortices were trimmed and cut into small pieces and processed for immunoelectron microscopy to visualize anti-ferritin Ab, rat C3 and rat C5b–9 complex. The non-perfused right kidneys were used as internal controls.

For immunoelectron microscopic examination, renal cortices were fixed by immersion for 4 h in 0.1 M phosphate-buffered 4% freshly prepared paraformaldehyde, pH 7.4, at 4°C, dehydrated in an ethanol series and embedded in Lowicryl K4 M (Chemische Werke Lowi, Waldkraiburg, Germany) according to the method of Carlemalm et al. [4]. The ultrathin sections, mounted on nickel grids, were incubated for 15 min in 0.02 M Tris-HCl, pH 7.0, containing 0.1% bovine serum albumin, then incubated with: (1) rabbit anti-rat IgG diluted 1:500 in Tris-HCl (E-Y Laboratories, San Mateo, Calif.); (2) rabbit anti-rat C3 diluted 1:1000 in Tris-HCl (Cappel Laboratories, West Chester, Pa.) for 2 h, followed by goat anti-rabbit IgG 10-nm colloidal gold conjugate diluted 1:10 in Tris-HCl (Janssen Life Science Products, Olen, Belgium) for 30 min at room temperature; or (3) monoclonal mouse anti-C5b-9 IgG (15 μg/ml of 2A1, kindly provided by Dr. Couser; Schulze et al. [25]), followed by affinity purified goat anti-mouse IgG diluted 1:500 in Tris-HCl (Cappel), which was preabsorbed with rat IgG, and finally rabbit anti-goat IgG 10-nm colloidal gold conjugate di-

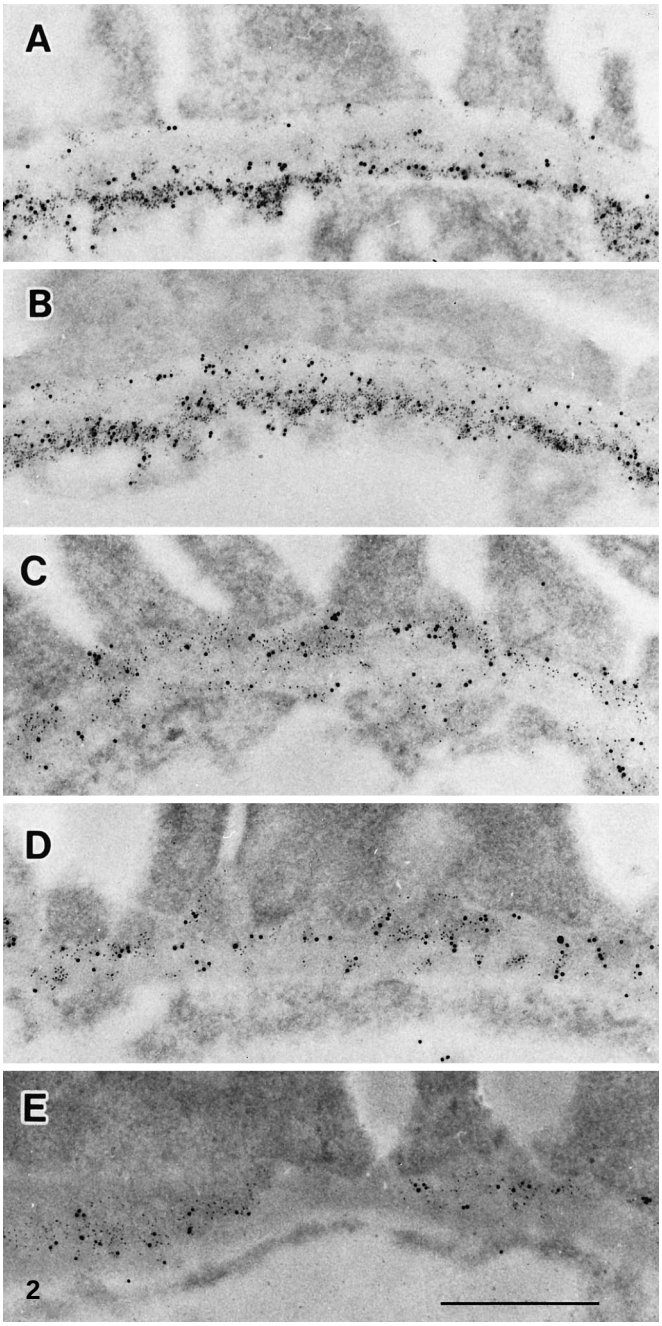

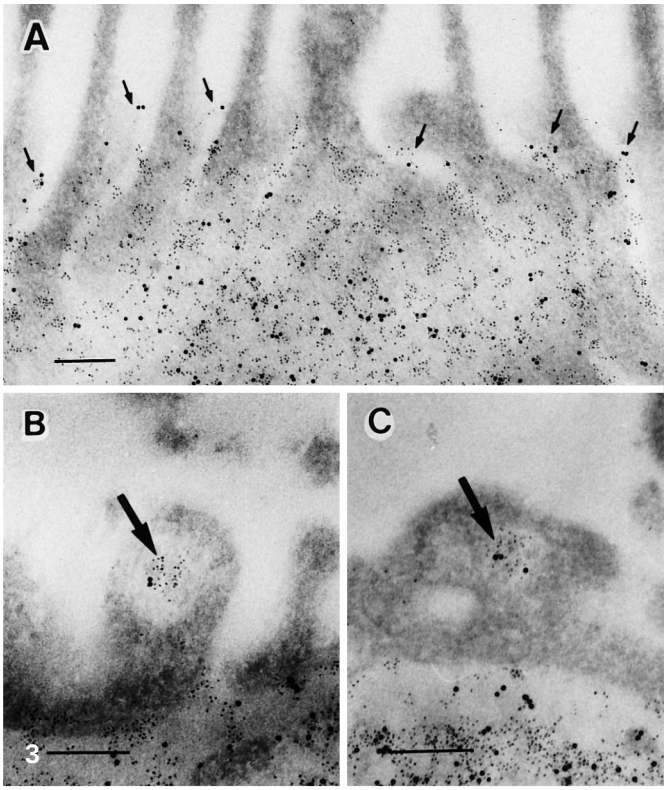

Fig. 2 Immunoelectron micrographs of the GBM of nephritic rats. Localizations of rat anti-ferritin Ab (*large particles*) and ferritin (*small particles*) on GBM are shown at **A** 15 min, **B** 2 h, **C** 1 day, **D** 2 days, **E** 7 days. Note that Ag and Ab shift from the subendothelial to subepithelial region with time, maintaining similar patterns of distribution. ×40,000, *bar* 0.5 μm

Fig. 3A–C Immunoelectron micrographs of rat anti-ferritin Ab (*large particles*) and ferritin (*small particles*). Bars 0.2 μm. **A** Arrows indicate Ag and Ab accumulated at the inter-podocyte space, nondistorted foot processes (2 h). ×40,000. **B**, **C** The epithelial cells contain Ag–Ab complex (*arrows*) in vacuole (6 h). ×54,000

luted 1:10 in Tris-HCl (Janssen). The sections were then washed with Tris-HCl buffer, rinsed three times with distilled water and air-dried. To confirm immunospecificity, the first antibody was omitted. Staining with 2% uranyl acetate for 10 min was conducted prior to observation under a JEM-200CX electron microscope (JEOL, Tokyo, Japan). Rat IgG, C3 and the C5b–9 complex were visualized by immunoelectron microscopy as 10-nm colloidal gold particles; CF was also visible as 5.5-nm particles.

For each antiserum, three or more glomeruli were observed. The density of Ag and the intensity of gold labelling for Ab, C3 and C5b–9 in the left kidneys of nephritic rats were assessed semiquantitatively on a scale of – to +++; the following areas: subendothelium, lamina densa (LD), subepithelium, inter-podocyte space, epithelium and mesangium, were estimated separately. The degree of recruitment of platelets, PMNs and monocytes in capillary lumina was also assessed semiquantitatively on a scale of – to +++.

Results

Urinary protein excretion increased to 42.0 ± 7.2 mg/24 h (means ± SD) on day 1 and reached its maximum level (78.0 ± 17.4 mg/24 h, means ± SD) on day 7. Abnormal proteinuria (> 10.0 mg/24 h) was not observed in rats prior to CF perfusion.

At 15 min, large amounts of both CF (Ag) and rat IgG (presumably anti-ferritin Ab) were detected in the subendothelial space of the GBM in the left kidneys (Fig. 2A). At this time small amounts of both Ag and Ab were also seen in the subepithelial space and beneath the slit membrane (Fig. 2A). With time, Ag and Ab migrated to the

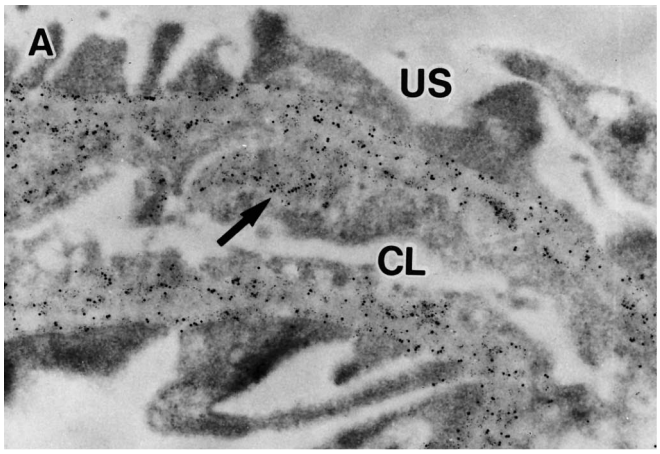

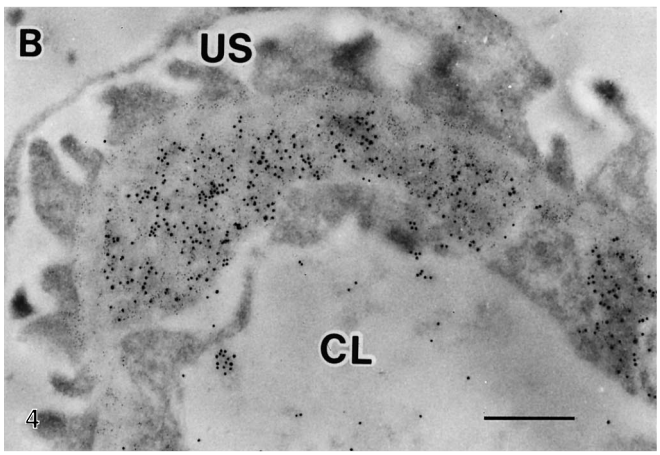

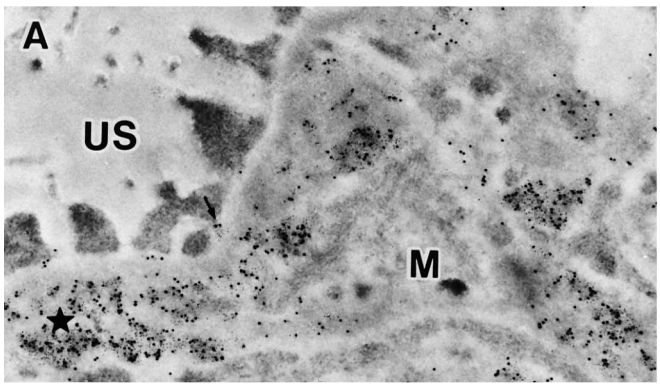

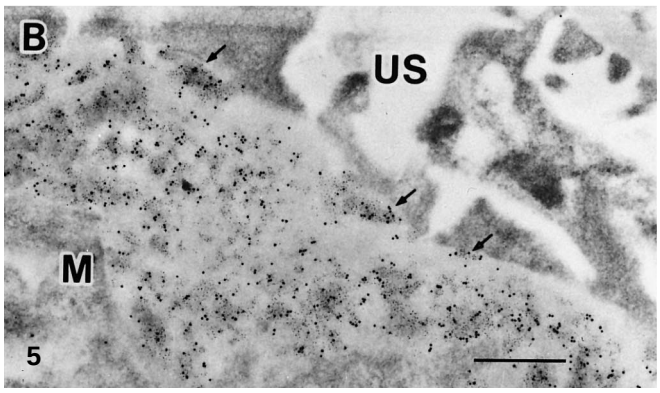

Fig. 4A, B Immunoelectron micrographs of the GBM of nephritic rats at day 1. ×22,500. **A** Co-localization of ferritin (*small particles*) and anti-ferritin Ab (*large particles*) within the entire width of the GBM and large subendothelial IC formation (*arrow*). **B** Large subendothelial deposits containing ferritin (*small particles*) and anti-rat C3 Ab (*large particles*). *CL* capillary lumen, *US* urinary space. *Bar* 0.5 μm

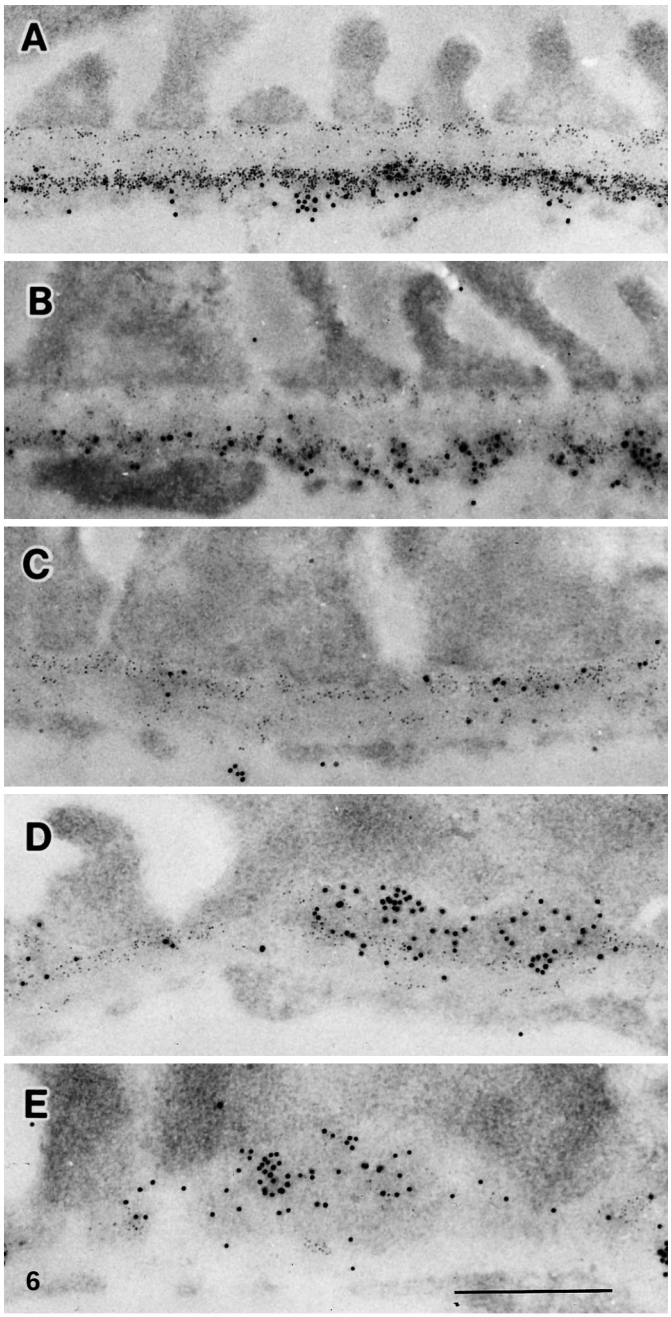

Fig. 5A, B Immunoelectron micrographs of mesangial regions. ×22,500. **A** Rat anti-ferritin Ab (*large particles*) and ferritin (*small particles*) are co-localized in the mesangial matrix adjacent to the subendothelial region (*asterisk*) of the GBM at day 1. Small subepithelial IC in mesangial region are also seen (*arrow*). **B** Both in the mesangial matrix and in the subepithelial region, the size and number of anti-ferritin Ab (*large particles*) and ferritin (*small particles*) increased slightly at day 7 (*arrows*). *M* mesangial cell, *US* urinary space. *Bar* 0.5 μm

Fig. 6 Immunoelectron micrographs of the GBM of nephritic rats, showing sequential localizations of rat C3 (*large particles*) and ferritin (*small particles*) on GBM at **A** 15 min, **B** 2 h, **C** 1 day, **D** 2 days, **E** 7 days. From 15 min to 2 h, C3 is found in the subendothelium together with ferritin, and from 1 day C3 appears in the subepithelium together with ferritin, which has become incorporated into the IC. ×40,000, *bar* 0.5 μm

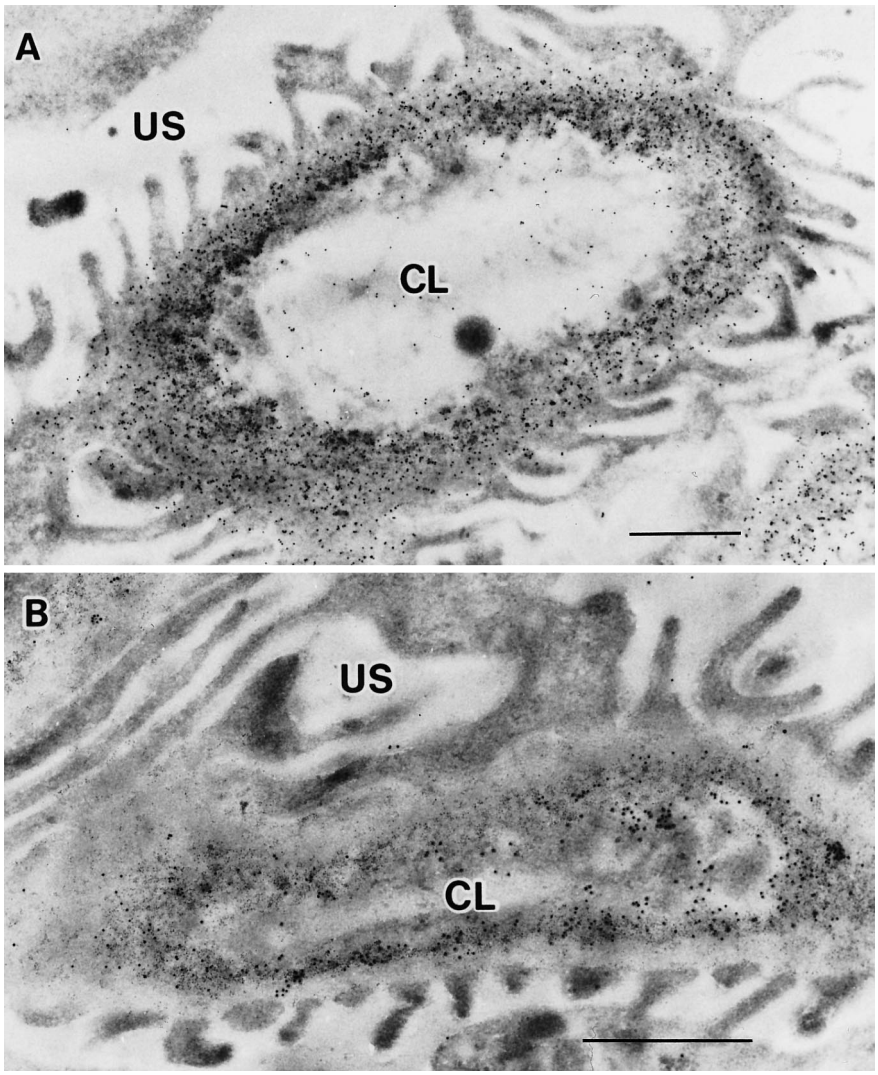

Fig. 7A, B Immunoelectron micrographs of oblique section from nephritic rat at 2 h. Note localization of rat anti-ferritin Ab (**A** *large particles*), rat C3 (**B** *large particles*) and ferritin (**A**, **B** *small particles*). Many rat anti-ferritin Ab molecules are present in the lamina densa, along with ferritin (**A**), but C3 remains in the subendothelial region together with ferritin (**B**). *CL* capillary lumen, *US* urinary space. **A** ×15,000, B ×22,500, *bars* 1.0 μm

subepithelial side, showing similar patterns of distribution at any given time point (Fig. 2). From 2 h to 1 day, many Ag and Ab particles appeared in the LD (Fig. 2B, C). Most Ab was located close to Ag particles in the LD (Fig. 2B, C and Fig. 7A) and aggregated Ag alone was never found within the LD. Within 1 day, Ag and Ab were found to be accumulated in the inter-podocyte space beneath non-distorted foot processes (Fig. 3A). This finding was most prominent at 6 h, at which time some epithelial cells were found to contain Ag and Ab in vacuoles (Fig. 3B, C). At day 1 the distribution of Ag and Ab varied from loop to loop (Fig. 2C and Fig. 4A), even within the same glomerulus. In some loops Ag–Ab complexes were predominant in the subendothelial space (Fig. 4), while in other loops Ag–Ab complexes were found predominantly in the subepithelial space (Fig. 2C). In some loops large subendothelial Ag–Ab complexes were observed at day 1 (Fig. 4A). After 2 days, Ag–Ab complexes were found in the subepithelial space in most capillary loops of glomeruli (Fig. 2D, E).

In the mesangium Ag and Ab were also observed adjacent to the subendothelial region of the GBM (Fig. 5A) after 2 h. These deposits increased slightly in number with expansion of the mesangial area (Fig. 5B), and subepithelial Ag and Ab in mesangial GBM also increased (Fig. 5). Ag and Ab were not observed in mesangial cells or at the vascular pole of the mesangium.

C3 was found in the subendothelial space in the vicinity of Ag at 15 min (Fig. 6A). During the passage of Ag and Ab through the LD from 2 h to 1 day, only a few particles of C3 were seen in the LD (Fig. 6B, C and Fig. 7B). After 1 day, C3 was seen distinctly in the aggregated subepithelial deposit containing Ag, while subendothelial C3 decreased with the disappearance of the Ag and Ab (Fig. 2C, D, E and Fig. 6C, D, E). After 2 days, C3 was seen prominently in the subepithelial region (Fig. 6D, E). C3 was not found in the epithelial cells.

Very little C5b–9 complex was found at the subendothelial site of Ag and Ab deposition (Fig. 8A, B). No C5b–9 complex attached to the endothelial cell membrane was found. After 1 day, C5b–9 complex was detected in the subepithelial Ag and Ab aggregation and in membrane vesicles in the epithelial cells (Fig. 8C, D).

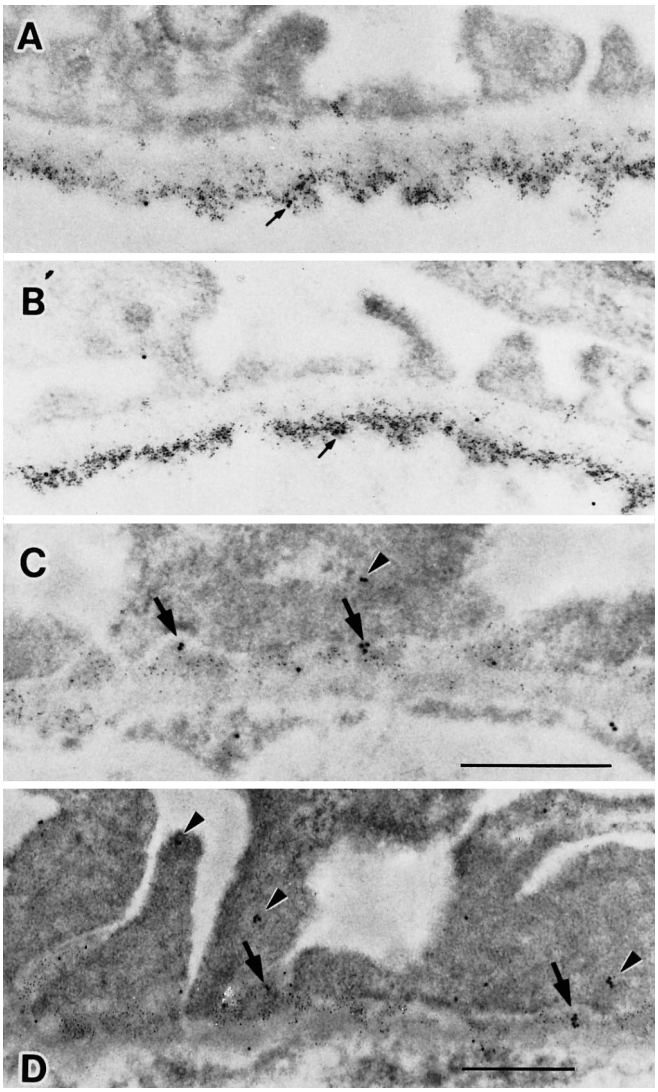

Fig. 8 Immunoelectron micrographs of the GBM of nephritic rats. Sequential localization of rat C5b–9 complex (*large particles*) and ferritin (*small particles*) on GBMs at **A** 15 min, **B** 2 h, **C** 1 day, **D** 7 days. Few C5b–9 complexes were seen in the subendothelial region (*small arrows*), and from day 1 onwards, C5b–9 complexes were found in the subepithelium with ferritin (*large arrows*). Some C5b–9 complexes are seen in the membrane vesicles in the epithelial cells (*arrowheads*). **A–C** ×40,000, **D** ×30,000, *Bars* 0.5 μm

However, no C5b–9 complex attached to the epithelial cell membrane was observed. C3 and C5b–9 were also found in aggregated mesangial immune deposits.

From 15 min to 2 h after induction of nephritis numerous platelets accumulated in some capillary lumina. Some of these appeared to be in contact with subendothelial Ag–Ab complexes (Fig. 9A). Focal endothelial cell denudation and swelling were seen at this time. From 2 h to 1 day there was significant PMN and monocyte infiltration into capillary lumina, the former being more prominent. The cytoplasmic processes (pseudopods) of PMNs and monocytes were in direct contact with endothelial cells and subendothelial immune deposits (Fig. 9B, E). Granules containing Ag, Ab and C3 could be seen in intracytoplasmic vacuoles of these PMNs, but rarely in monocytes (Fig. 9B–E). This endocytotic process was also seen at 15 min. The findings described above are summarized by semiquantitative assessment in Table 1.

In the non-perfused right kidneys of nephritic rats (internal control), virtually no immunoreactants were found. On immunoelectron microscopic observation, very few gold particles were seen in the glomeruli of nephritic rats when first antibodies were omitted.

Discussion

We have examined the ultrastructural localization of Ag, Ab, C3, C5b–9 complex and inflammatory cells in active in situ IC glomerulonephritis induced with CF.

Initially Ag and Ab were deposited in the subendothelial space and then passed through the GBM. C3 was found in Ag and Ab aggregations in the subendothelial space but was not found in the LD when Ag and Ab passed through the GBM. Later C3 reappeared in the subepithelial space in the vicinity of Ag–Ab complex. Only a few C5b–9 deposits were found in the subendothelial space when Ag, Ab and C3 were found in the subendothelial space, but later significant amount of C5b–9 was observed in the subepithelial space with Ag–Ab complexes.

These findings suggest the following. Ab first bound to Ag in the lamina rara interna, where Ag–Ab aggregates (IC formation) appeared and activated complement. The activation of complement in the subendothelial space may contribute to the translocation of Ag–Ab complexes through the GBM, since the depletion of complement lessened this translocation [11]. The activated C3 split products in the subendothelial space were dissociated from Ag–Ab complexes. Smaller Ag–Ab complex then left the subendothelial region and passed through the GBM. The kinetics of Ag and Ab transfer across the GBM in active in situ IC nephritis in this experiment was essentially the same as in passive in situ IC nephritis [10]. Ag–Ab deposits might also be formed directly at outer side of the GBM, since some Ag–Ab aggregates were noted at the subepithelial side of the GBM after as little as 15 min and 2 h. The above events in the development of the subepithelial IC formation seem to be essential in models of both active and passive in situ IC nephritis employing cationic Ag.

The C5b–9 membrane attack complex is considered to be a major mediator of IC-mediated glomerular injury through glomerular epithelial cell damage [6, 7, 15]. However, little is known about the formation and the role of C5b–9 complex in the subendothelial region. In contrast to C3, very small amounts of C5b–9 complex were found in the subendothelial region in this experiment, and no evidence showing that the C5b–9 complex attached to the endothelial cell membrane was obtained. This might reflect the role of the alternative complement

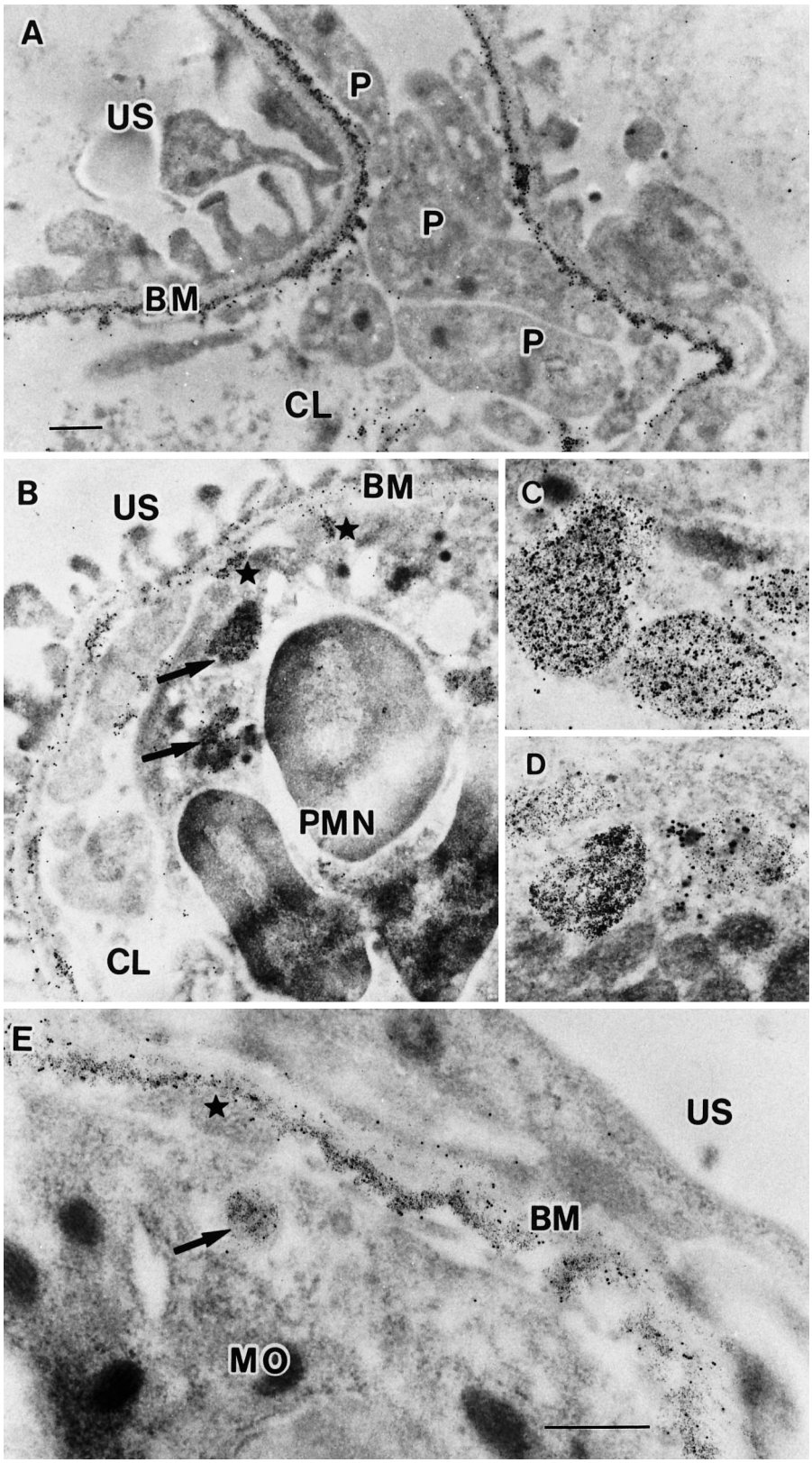

Fig. 9 Immunoelectron micrographs of glomerulus from nephritic rats at 2 h, showing localizations of **A**, **D** rat C3 (*large particles*), **B**, **C**, **E** rat anti-ferritin Ab (*large particles*) and **A–E** ferritin (*small particles*). **A** Marked platelet (*P*) accumulation is seen in the capillary lumen, some patelets appearing to be in contact with IC localized in the subendothelium. **B** A polymorphonuclear leucocyte (PMN), which has endocytosed ICs (*arrows*), appears to be in direct contact with IC localized in the subendothelium (*asterisks*). **C**, **D** Intracytoplasmic vacuoles of a polymorphonuclear leucocyte containing (**C**) ferritin and anti-ferritin Ab and **D** intracytoplasmic vacuoles of a monocyte containing ferritin and anti-rat C3. **E** A monocyte (*MO*), in direct contact with IC in the subendothelium (*asterisk*) is engulfing IC (*arrow*). *CL* capillary lumen, *US* urinary space, *BM* basement membrane. **A, B** ×15,000, **C–E** ×30,000, *bars* 0.5 μm

pathway. C3 activated by Ag–Ab complex might solubilize ICs [8, 20] and stimulate the translocation of ICs [11], and the activation of C3 would not then be followed by C5b–9 formation. A contribution of the membrane attack complex to endothelial cell damage cannot be excluded, since focal endothelial cell denudation was seen in the current model. C5b–9 complex was found both in the subepithelial ICs and in membrane vesicles in the epithelial cells. However, the existence of IC and C5b–9 in the subepithelial space in this model does not neces-

Table 1 Time course of localization of Ag, Ab, complement and inflammatory cells

Time		15 min	2 h	6 h	Day 1	Day 2	Day 7
Ag	Subendo	+++	+++	++	+(+++)	–	–
	Intra-GBM	±	+(++)	+(++)	+(++)	(±)	(±)
	Subepi	+	+(++)	++	++(+++)	+++	+++
	Inter-pod	±	±(+)	+	±	–	–
	Epi	–	–	(+)	–	–	–
	Mes	±	±(+)	+	+	+(++)	+(++)
Ab	Subendo	+++	+++	++	+(+++)	–	–
	Intra-GBM	±	+(++)	+(++)	+(++)	(±)	(±)
	Subepi	+	+(++)	++	++(+++)	+++	+++
	Inter-pod	±	±(+)	+	±	–	–
	Epi	–	–	(+)	–	–	–
	Mes	–	+	+	+	+(++)	+(++)
C3	Subendo	++	+++	++	±(+)	–	–
	Intra-GBM	–	–	–	–	–	–
	Subepi	–	–	–	±(+)	++(+++)	+++
	Inter-pod	–	–	–	–	–	–
	Epi	–	–	–	–	–	–
	Mes	–	±	+	+	+(++)	+(++)
C5b-9	Subendo	(±)	(±)	–	–	–	–
	Intra-GBM	–	–	–	–	–	–
	Subepi	–	–	–	+	+(++)	+(++)
	Epi	–	–	–	(+)	+	+
	Mes	–	±	±	±(+)	+	+
Plt		+++	++	±	±	–	–
PMN		+	+++	++	+(++)	(±)	(±)
Mo		(±)	+	+	+	±(+)	±(+)

(*Subendo* subendothelial region, *Subepi* subepithelial region, *Inter-pod* inter-podocyte space, Epi epithelium, *Mes* mesangial region, Plt platelet in capillary lumen, *PMN* polymorphonuclear leucocyte in capillary lumen, *Mo* monocyte in capillary lumen, +++ strong and massive, ++ moderate and frequent, + mild and infrequent, ± weak and very infrequent, – almost negative, ( ) segmental finding

sarily indicate a contribution of C5b–9 to the epithelial cell damage or to the development of proteinuria, and we did not find C5b–9 complex attached to the epithelial cell membrane. The contribution of the C5b–9 membrane attack complex to the development of epithelial cell damage has been defined [6, 7, 15], and Kerjaschki et al. [15] have demonstrated C5b–9 complex on the subepithelial cell membrane in passive Heymann nephritis. These authors also reported that C5b–9 was observed in the subepithelial deposits, as well as in membrane vesicles in epithelial cells in passive in situ IC nephritis employing cationic IgG. However, it is unclear whether the C5b–9 complex attached to the epithelial cell membrane, because of the limitations of the technique used.

In this study Ag–Ab complexes without C3 were often seen at the interspaces of the foot processes within 1 day, and in some epithelial vacuoles at 6 h. These findings indicate that non-aggregated IC too small to activate complement might pass through the slit membrane into the urinary space or be taken up into the epithelial cells via endocytosis [22, 27]. From 1 day onwards the Ag–Ab complexes aggregated in the subepithelial space were large enough to activate complement and ensure persistence. Ag–Ab aggregation in this space was associated with retraction of foot processes. C3 in the subepithelial region might either come from the circulation or be locally synthesized by the epithelial cells, as reported by Sacks et al. [23], but the mechanisms of IC retention in the subepithelial space and the fate of subepithelial IC remain to be clarified.

Ag–Ab complexes were also found in the mesangial matrix adjacent to the subendothelial region after 2 h increasing slightly in number with expansion of the mesangial area thereafter. Modest subepithelial IC formation in the mesangial GBM also developed. Ag and Ab were observed 15 min after the perfusion of Ag in the subendothelial area but not in the mesangium, and no immunoreactants were found in the right kidney. These findings indicate that the contribution of circulating IC was negligible in this model and that mesangial IC deposits in the left kidney seemed to be derived from subendothelial IC. Oite et al. [21] also reported paramesangial deposition of CF in active in situ IC nephritis and suggested that some of the CF located subendothelially is transported into the mesangium as part of its clearing function. However, the precise kinetics of IC in the mesangial region is still unclear. Large-latticed IC in the subendothelial space could be swept laterally into the mesangial region, as suggested by Makino et al. [16]. The clearance of subendothelial IC seems to be a minor event, since in comparison with IC in the peripheral GBM, subepithelial IC in the mesangial GBM were small. The hypothesis that ICs were removed by mesangial cell phagocytosis [17] or transported to the vascular pole of the mesangium could not be confirmed by the current experiment.

Generally the formation of subendothelial immune deposits was accompanied both by inflammatory cell infiltration and by complement activation [9, 24]. The accumulations of platelets and PMN are reported to be complement dependent in concanavalin A-anti-concanavalin A-induced nephritis [14]. In agreement with this hypothesis, the accumulation of platelets and PMN was observed 15 min after the induction of active in situ IC nephritis, when C3 deposition in the subendothelial

space was found. This does not exclude the possibility that complement activation is not essential for PMN accumulation [29]. The accumulated platelets, PMN, and monocytes were in direct contact with endothelial cells or subendothelial IC, and PMN and monocytes contained Ag, Ab and C3 in intracytoplasmic vacuoles. These inflammatory cells may therefore function as phagocytic scavengers and eliminate subendothelial immune reactants [5, 26, 28]. Since platelet influx has been seen in many other models of IC-mediated glomerulonephritis [2, 9, 12–14, 18, 19], it is probably a feature of nephritis in which ICs form primarily on the luminal side of the glomerular capillary wall. The exact roles of inflammatory mediator systems and their interrelationship in this active in situ IC nephritis remain to be clarified.

Most ICs formed initially at the subendothelial side rapidly formed lattices of a size that activated C3, They were then translocated to the subepithelial space as small-latticed ICs. The ability of C3 to solubilize ICs in the subendothelial region may be important in this process. The endocytosis of subendothelial ICs by PMN and/or monocyte and the movement of ICs to mesangial matrix may also contribute to the clearance of subendothelial IC.

Acknowledgement We are indebted to Dr. W.G. Couser for the generous gift of monoclonal mouse anti-C5b–9 IgG.

References

1. Barnes JL, Venkatachalam MA (1985) The role of platelets and polycationic mediators in glomerular vascular injury. Semin Nephrol 5:57–68
2. Barnes JL, Camussi G, Tetta C, Venkatachalam M (1990) Glomerular localization of platelet cationic proteins after immune complex-induced platelet activation. Lab Invest 63:755–761
3. Bradford MM (1976) A rapid and sensitive method for the quantitation of microgram quantities of protein utilizing the principle of protein-dye binding. Anal Biochem 72:248–254
4. Carlemalm E, Garavito RM, Villiger W (1982) Resin development for electron microscopy and an analysis of embedding at low temperature. J Microsc 126:123–143
5. Cochrane CG, Weigle WO, Dixon FJ (1959) The role of polymorphonuclear leucocytes in the initiation and association of the Arthus vasculitis. J Exp Med 110:481–494
6. Couser WG (1985) Mechanisms of glomerular injury in immune complex disease. Kidney Int 28:569–583
7. Couser WG, Baker PJ, Adler S (1984) Complement and the direct mediation of immune glomerular injury: a new perspective (editorial review). Kidney Int 28:879–891
8. Czop J, Nussenzweig V (1976) Studies on the mechanism of solubilization of immune precipitates by serum. J Exp Med 143:615–630
9. Fries JWV, Mendrick DL, Rennke HG (1988) Determinants of immune complex-mediated glomerulonephritis. Kidney Int 34:333–345
10. Fujigaki Y, Nagase M, Honda N (1993) Intraglomerular basement membrane translocation of immune complex (IC) in the development of passive in situ IC nephritis of rats. Am J Pathol 142:831–843
11. Fujigaki Y, Batsford SR, Bitter-Suermann D, Vogt A (1995) Complement system promotes transfer of immune complex across glomerular filtration barrier. Lab Invest 72:25–33
12. Gabbiani G, Badonnel MC, Vassalli P (1975) Experimental focal glomerular lesions elicited by insoluble immune complexes. Ultrastructural and immunofluorescent studies. Lab Invest 32:33–45
13. Golbus SM, Wilson CB (1979) Experimental glomerulonephritis induced by in situ formation of immune complexes in glomerular capillary wall. Kidney Int 16:148–157
14. Johnson RJ, Alpers CE, Pruchno C, Schulze M, Baker PJ, Pritzl P, Couser WG (1989) Mechanisms and kinetics for platelet and neutrophil localization in immune complex nephritis. Kidney Int 36:780–789
15. Kerjaschki D, Schulze M, Binder S, Kain R, Ojha PP, Susani M, Horvat R, Baker PJ, Couser WG (1989) Transcellular transport and membrane insertion of the C5b-9 membrane attack complex of complement by glomerular epithelial cells in experimental membranous nephropathy. J Immunol 143:546–552
16. Makino H, Lelongt B, Kanwar YS (1988) Nephritogenicity of proteoglycans. III. Mechanism of immune deposit formation. Kidney Int 34:209–219
17. Mancilla-Jimenez R, Bellon B, Kuhn J, Belair MF, Rouchon M, Druet P, Bariety J (1982) Phagocytosis of heat-aggregated immunoglobulins by mesangial cells. An immunoperoxidase and acid phosphatase study. Lab Invest 46:243–253
18. Matsuo S, Fukatsu A, Taub ML, Coldwell PRB, Brentjens JR, Andres G (1987) Glomerulonephritis induced in the rabbit by antiendothelial antibodies. J Clin Invest 79:1798–1811
19. Matsuo S, Yoshida F, Yuzawa Y, Hara S, Fukatsu A, Watanabe Y, Sakamoto N (1989) Experimental glomerulonephritis induced in rats by a lectin and its antibodies. Kidney Int 36:1011–1021
20. Miller GW, Nussenzweig V (1975) A new complement function. Solubilization of antigen-antibody aggregates. Proc Natl Acad Sci USA 72:418–422
21. Oite T, Shimizu F, Suzuki Y, Vogt A (1985) Ultramicroscopic localization of cationized antigen in the glomerular basement membrane in the course of active, in situ immune complex glomerulonephritis. Virchows Arch [B] 48:107–118
22. Rantala I (1981) Glomerular epithelial cell endocytosis of immune deposits in the nephrotic rat. Nephron 29:239–244
23. Sacks SH, Zhou W, Andrews PA, Hartley B (1993) Endogenous complement C3 synthesis in immune complex nephritis. Lancet 342:1273–1274
24. Salant D, Adler S, Darby C, Capparell NJ, Groggel GC, Feintzeig ID, Rennke HG, Dittmer JE (1985) Influence of antigen distribution on the mediation of immunological glomerular injury. Kidney Int 27:938–950
25. Schulze M, Baker PJ, Perkinson DT, Johson RJ, Ochi RF, Stahl RAK, Couser WG (1989) Increased urinary excretion of C5b-9 distinguishes passive Heymann nephritis in the rat. Kidney Int 35:60–68
26. Schwartz BS, Edgington TS (1981) Immune complex induced human monocyte procoagulant activity. J Exp Med 154:892–906
27. Sharon Z, Schwartz MM, Pauli BU, Lewis EJ (1978) Kinetics of glomerular visceral epithelial cell phagocytosis. Kidney Int 14:526–529
28. Steffelaar JW, Graaff-Reitsma CBDE, Feltkamp-Vroom TM (1976) Immune complex detection by immunofluorescence on peripheral blood polymorphonuclear leucocytes. Clin Exp Immunol 23:272–278
29. Thaiss F, Batsford S, Mihatsch MJ, Heitz PV, Bitter-Suermann D, Vogt A (1986) Mediator systems in a passive model of in situ immune complex glomerulonephritis. Lab Invest 54:624–635
30. Vogt A, Rohrbach R, Shimizu F, Takamiya H, Batsford S (1982) Interaction of cationized antigen with rat glomerular basement membrane. In situ immune complex formation. Kidney Int 22:27–35